

# Exploiting Diluted Bioethanol Solutions for the Production of Ethylene: Preliminary Process Design and Heat Integration

Ilenia Rossetti<sup>a\*</sup>, Antonio Tripodi<sup>a</sup>, Elnaz Bahadori<sup>a</sup>, Gianguido Ramis<sup>b</sup>

<sup>a</sup> Chemical Plants and Industrial Chemistry Group, Dip. Chimica, Università degli Studi di Milano, CNR-ISTM and INSTM Unit Milano-Università, via C. Golgi 19, 20133 Milano, Italy.

<sup>b</sup> Dip. Ing. Chimica, Civile ed Ambientale, Università degli Studi di Genova and INSTM Unit Genova, via Opera Pia 15, Genoa, Italy  
 ilenia.rossetti@unimi.it

Several activity tests on a zeolite-based catalyst for the ethanol to ethylene dehydration reaction are used to outline the stoichiometry of 4 reactions describing the observed outcome. The heat and mass balances of a reactor were calculated. The thermal input was mainly sustained with a standard product-to-feed heat exchange. Upstream, two possible strategies of ethanol-water beer concentration were compared, namely a single stage flash and a small column, yielding respectively a 3:1 water:ethanol mixture and a slightly diluted azeotrope. The external heat input needed for the separation unit, the feed heating up to the reaction temperature and the reaction upkeep are compared. A flow diagram for the hot utility is then designed, converting part of the water of the beer into superheated steam that gives also electric power. The conceptual design of an ethanol to ethylene plant is therefore available to exploit bioethanol solution with different water/ethanol ratios, with different ethanol purification routes with variable heat input and energy recovery.

## 1. Introduction

As the plastic world demand grows, followed closely by the polyethylene one ([pubs.acs.org/cen/coverstory/84/pdf/8428production.pdf](https://pubs.acs.org/cen/coverstory/84/pdf/8428production.pdf), 2006), strategies to base ethylene production on renewable sources become more and more interesting (Posen & al., 2014; Rossetti & al., 2017a; Ramis & al., 2017). The long known and exploited ethanol – ethylene reversible reaction (Paik & al., 1938; Kodama & al., 2005) can take advantage of the high activity of zeolite-based catalysts (Phillips & al., 1997; Rossetti & al., 2017b; Gayubo & al., 2010), or other, variously promoted, acidic oxides (Kagymanova & al., 2011). On the other hand, a large scale process relying on presently marketed bio-ethanol as feed would likely lead to a non-competitive product, due to the minimum ethanol prices required from the fermentation plants management (Aden & al., 2002), besides the involved quantities (Fan & al., 2013; Althoff & al., 2013).

The key point to start exploiting bio-ethanol as a green and renewable source for ethylene is the integration of this process as the second stage (or as a part) of a fermentation plant itself on one side, and, possibly, as the first step of a polymerization process on the other side (Fan & al., 2013). In this way, part of the ethanol output would turn into a more valuable product and an alternative renewable platform with respect to biomass gasification would be established (Posen & al., 2014). In this view, the possibility to use diluted bioethanol instead of the marketed fuel-grade (or even azeotropic) product is very interesting, because the raw material for ethylene would be much less expensive and the dehydration catalysts now available do not suffer deactivation by water, while they are kept clean from coke in excess steam. Therefore, based on the experimentally determined ethylene productivity, we have compared different simulated plants, which integrate an ethylene production unit into an ethanol production plant. Different purification strategies have been compared for bioethanol, taking advantage of the possibility to use diluted ethanol streams. A review of several present-day bio-ethylene plants, indicating a range from 60,000 to 200,000 t/y (Fan & al., 2013), suggested to fix a demo-scale size of 700-800 t/y as the basis for this work.

## 2. Calculation Methods

To compare different strategies of the raw material and energy supply management, mass and heat balances have been implemented in the process simulation software Aspen Plus<sup>®</sup>. The flowsheets used for the calculations are reported in Figures 1- 3, showing a bare reactive section, a reactive section preceded by a feed purification column and a reactive-purification section with a steam energy cycle, respectively. Since this work is primarily concerned with the ethylene yield respect to different possible bioethanol feeds, the purification part of the plant has been omitted in schemes and 1 and 2, while it has been lumped in just three main blocks in scheme 3. All the calculations were done using the following combination of thermodynamic models: Redlich-Kwong-Soave Equation of State (EoS) for the species in gaseous phase or at high pressure, Non-Random Two Liquids / Redlich-Kwong EoS for mixed phases at low pressure (in this case, however, supercritical components as ethylene and ethane are treated via their Henry constants with respect to water).

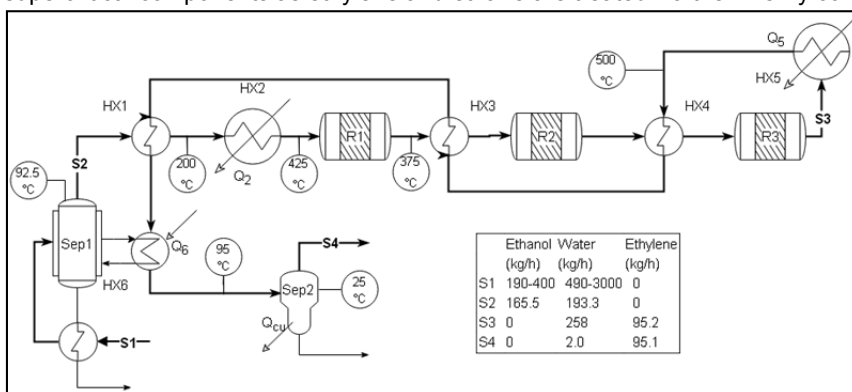


Figure 1: Basic scheme for the ethanol feed, reactor and ethylene-water separation. The flash separator temperature corresponds to the achieved mass ratio in the S2 stream.

### 2.1 Reactive section

The ethanol-ethylene process is built upon the activity tests performed on a HALBEA material (BEA zeolite in acidic form with Si/Al=17 mol/mol), loaded with 0.5 wt% Ni. The details on the catalyst performance can be found elsewhere (Rossetti & al., 2017a). We report in Table 1 the data used (two other data sets, at a higher / lower temperature respectively, have been discarded because they showed lower selectivity / conversion). Since the tests were run at a constant GHSV, the reactions can be described with their yield only and cannot be implemented in a PFR-type block. Kinetic testing is currently in progress to fix this point.

Table 1: Activity data for the catalyst described in used reference [3].

Run	T (°C)	H <sub>2</sub> O:C <sub>2</sub> H <sub>6</sub> O (mol/mol)	Conversion (%)	Yield (%)			
				C <sub>2</sub> H <sub>4</sub>	C <sub>2</sub> H <sub>4</sub> O	CO <sub>2</sub>	C <sub>2</sub> H <sub>6</sub>
1	400	3	100	97.15	2.3	0.4	-
2	400	Pure EtOH	100	97.3	2.2	0.2	0.2

The catalyst is able to reach full conversion, with a very good selectivity to ethylene, both with pure and diluted ethanol, without being deactivated by water. Below 500 °C the steam reforming reaction is not important, but it is a common alternative path on acidic-oxides (Rossetti & al., 2015) and has to be taken into account to explain the full oxidation shown by CO<sub>2</sub>. Ethane, on the other hand, is likely the product of ethylene reduction. The following stoichiometry is proposed and implemented in the Aspen Plus<sup>®</sup> 'Stoichiometric' reactor:



The reactor is divided into three beds in order to represent the re-heating stages needed by an actual unit. Each of them, however, is not completely adiabatic but is assigned a heat duty such as to keep the temperature drop within 50 °C (*i.e.* ±25 °C around the chosen reactor temperature of 400 °C): in this way, reaction conditions close to the lab-test ones can be studied in relation to an actual reactor without increasing too much the simulation complexity. Notice that the adopted stoichiometry is always based on ethanol, even

when the actual reacting species is probably another (e.g. reaction 4): this is of help, when dealing with the aforementioned ‘Stoichiometric’ block, because every reaction is then calculated independently and the mass balances can be adjusted much more easily – in our case, being ethanol the only C-containing reactant, this approach is fully justified –: the recalculated yields are different from the observed ones only in the cases of the non-observed species (methane and hydrogen), that are anyway in small quantities. With the conversion data available, the flow of ethanol required to meet the target productivity of ethylene is 165 kg/h.

## 2.2 Feeding section

Standing the catalyst capability to fully convert diluted ethanol and the beneficial effect of water against coke formation, the feeding section is designed to yield a mixture of 3 moles of water per mole of ethanol with a single flash separation block, kept at 92.5 °C according to the water-ethanol phase diagram as calculated by the NRTL-RK method (see also Becerra & al., 2017 for a calculation done with a different model). To obtain this vapor composition starting from differently diluted beers, the total mass flow of ethanol entering the separator block is varied manually while a ‘Design Specification’ convergence block automatically adjusts the relative gross water input (both these values have to be adjusted in order to satisfy the thermodynamic equilibrium condition while producing enough vaporized ethanol to meet the target ethylene yield). In this way, we can account for the heat duty needed to extract 165 kg/h of ethanol and 193 kg/h of water from hydroalcoholic solutions in a dilution range from 5 to 13 mol%, representing different stages and compositions of the fermentation broths actually managed in the bioethanol plants (Aden & al., 2002). The water excess is vaporized and routed through the reactors, until is separated in another flash block modeled according to the liquid-phase equilibrium at 25 °C: since the product mixture contains 1 mole of ethylene per 3 moles of water, the first species solubility is modeled with the Henry constant. See Table 2 for a summary of the input feed mixtures:

Table 2: Composition of the model hydro-alcoholic beers used in the simulation.

Case #	Beer feed (kg/h)		Ethanol feed (kg/h)		Ethanol dilution (mol / mol)
	Flash	Column	Flash	Column	
A	676	550	190	220	0.132
B	1065	1065	220	220	0.092
C	3398		400	220	0.049

In many cases, however, the catalysts are fed with pure or highly concentrated ethanol (Becerra & al., 2017; Mohsenzadeh & al., 2017; Cameron & al., 2012) and the bioethanol plants are equipped with an ethanol concentration section (Aden & al., 2002). Therefore, a different feeding section is designed as a single column that produces a nearly azeotropic ethanol-water vapor, in order to compare the mass balances and heat duties of the two solutions. The feed flow of ethanol is fixed at 220 kg/h and the different beer dilutions are represented varying the water flow only. In this way the distillate rate of the column can be kept fixed, which greatly increases the calculation stability passing from one case to the other. The other column specifications (20 trays, feed stage at the 15<sup>th</sup>, 176 kg/h of vapor distillate) have been optimized accordingly, to achieve a minimum ethanol mole fraction of 85 % in the distillate and the only parameter varied to cope with different beers was the reflux ratio.

## 2.3 Heat recovery section

The heat needed to vaporize the feed is supplied at the beer concentration unit (Sep1 or the column), while the thermal energy that compensates the dehydration enthalpy difference ( $\Delta_r H^0 = 43.4$  kJ/mol) is supplied at the reactor exit (block HX5 in Figures 1-3) and is distributed between the catalytic beds via a feed-to-product heat exchange network. The heat foreseen to keep each reactor section at  $400 \pm 25$  °C is counted in the duty  $Q_5$  of the product re-heater HX5. Notice that the temperature of the super-heated ethanol-water vapor exiting the first heater HX1 (200 °C) could be modified, leaving a different enthalpy content to be exchanged in the last heat economizer HX6, where the ethylene-water mixture cools down to 94-99 °C. This latter range of values represents the lowest temperatures possibly achievable if the product stream acts as hot utility for the beer flash or beer column units, on the basis of these separators behavior. Nevertheless, also in the case where the HX6 economizer is used to heat the service water feed (Figure 3), the hot side lowest temperature is not actually higher than its dew-point (93 °C for the diluted ethanol cases). This happens because, as water condenses, the heat released is so high with respect to the cold stream heat capacity that the internal pinch point of the exchanger is rapidly reached and crossover errors are issued. For this reason, in the cases where the full power integration is studied, this block is analyzed carefully splitting its calculation in as much as 50 zones (in countercurrent arrangement, with nested recursive calculation of the LMTD) and the lowest hot



turbines allow for a 10% loss respect to the isentropic ideal case. The residual heat of the MP steam is exchanged at 1 bar, because it is potentially exploitable to heat the flash separator ( $\Delta T = 7\text{ }^{\circ}\text{C}$ , with saturated fluids on both sides).

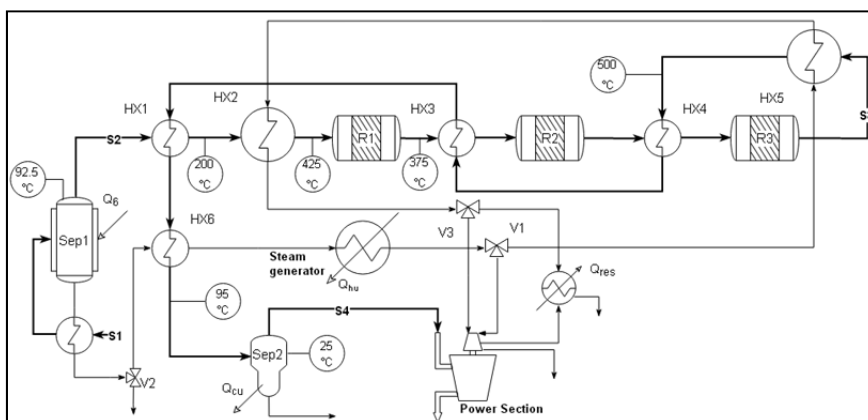


Figure 3: Basic scheme for the beer flash, reactor and ethylene-water separation with internal hot utility: not shown is the 'heat link' that transfer the duty  $Q_6$  to  $Q_{res}$ . Relevant mass flows are as in Figure 1. The higher steam temperature is  $640\text{ }^{\circ}\text{C}$ , the power section works between 35, 12 and  $0.1\text{ bar}$ .

Table 3: Heat duties for the case of feed concentrated with a single flash block. The number in parentheses indicate the higher temperatures (in  $^{\circ}\text{C}$ ) relative to the heat exchange.

Case #	Hot utility (external)			Heat sink	
	Beer flash (kW)	Feed heater (kW)	Product heater (kW)	Total (kW)	Separator (kW)
A	146 (93)	48 (425)	37 (500)	231	185 (25)
B	148 (93)	48 (425)	37 (500)	234	185 (25)
C	162 (93)	48 (425)	37 (500)	247	185 (25)

Table 4: Heat duties for the case of feed concentrated with a distillation column.

Case #	Hot utility (external)			Total (kW)	Heat sink		Column Reflux Ratio (mol/mol)
	Beer column (kW)	Feed heater (kW)	Product heater (kW)		Column condenser (kW)	Separator (kW)	
A	212 (91)	25 (425)	43 (500)	280	176 (78)	56 (25)	3.8
B	224 (94)	25 (425)	43 (500)	292	185 (78)	56 (25)	4.0
C	252 (96)	25 (425)	43 (500)	320	208 (78)	56 (25)	4.5

Table 5: Heat duties provided by boiling at different temperatures the recycled water extracted from the flash-concentrated beer.

Case #	Hot utility (recycled water)				Recycle water		Heat sink Separator (kW)
	Steam generator (kW)		Output power (kW)		(kg/kg)		
	$(T_h=760\text{ }^{\circ}\text{C})$	$(T_h=640\text{ }^{\circ}\text{C})$	$(T_h=760\text{ }^{\circ}\text{C})$	$(T_h=640\text{ }^{\circ}\text{C})$	$(T_h=760\text{ }^{\circ}\text{C})$	$(T_h=640\text{ }^{\circ}\text{C})$	
A	288	267	0.31	-10	0.99	0.99	185 (25)
B	288	305	0.78	3.9	0.44	0.50	185 (25)
C	300	316	0.11	2.9	0.11	0.12	185 (25)

#### 4. Conclusions

Considering a catalyst that is able to fully convert both diluted and pure ethanol, two different feeding strategies have been compared. The use of a distillation column would require on the average  $0.6\text{ kW per kg/h}$  of product more than in the case of a single flash block, but implies a 30% higher duty to the cold utility. The choice between the two options depends critically on the quantity of water that can successfully prevent the formation of coke on the acidic catalyst used. Supposing to use steam as hot utility for the process, the

thermal duties can be integrated with the foreseen power demand of a high pressure ethylene dehydration: a careful management of this section can indeed accomplish both tasks with a reasonable 20 % increase of the single-flash heat consumption and this performance is fairly stable even decreasing the superheating temperature. Even if the water recycle foreseen in this work should be properly reconsidered when real fermentation beers (not including just water and ethanol) are modelled, this calculation shows that the heat, power and mass balance integration of a bioethanol to pure ethylene process can be achieved without increasing excessively the plant energy demand. Moreover, very diluted fermentation beers could be used and concentrated to the water / ethanol ratio actually needed from the catalyst without the need of the azeotropic column.

## References

- Aden A., Ruth M., Ibsen K., Jechura J., Neeves K., Sheehan J., Wallace B., 2002, Lignocellulosic Biomass to Ethanol Process Design and Economics Utilizing Co-Current Dilute Acid Prehydrolysis and Enzymatic Hydrolysis for Corn Stover, Technical Report, National Renewable Energy Laboratory, Colorado.
- Althoff J., Biesheuvel K., De Kok A., Plet H., Ruitenbeek M., Spork G., Tange J., Wevers R., 2013, Economic Feasibility of the Sugar Beet-to-Ethylene Value Chain, *Chem. Sus. Chem.*, 6, 1625-1630, DOI: 10.1002/cssc.201300478.
- Becerra J., Figueredo M., Cobo M., 2017, Thermodynamic and economic assessment of the production of light olefins from bioethanol, *Journal of Environmental Chemical Engineering*, 5, 1554-1564, DOI: 10.1016/j.jece.2017.02.035.
- Cameron G., Le L., Levine J., Nagulapalli N., 2012, Process Design for the Production of Ethylene from Ethanol, Senior Design Reports (CBE), 39, Penn Libraries, [http://repository.upenn.edu/cbe\\_sdr/39](http://repository.upenn.edu/cbe_sdr/39).
- Fan D., Dai Der-J., Wu Ho-S., Eds., 2013, Ethylene Formation by Catalytic Dehydration of Ethanol with Industrial Considerations, *Materials*, 6, 101-115, DOI: 10.3390/ma601010.
- Gayubo A. G., Alonso A., Valle B., Aguayo A. T., Bilbao J., 2010, Kinetic Model for the Transformation of Bioethanol into Olefins over a HZSM-5 Zeolite Treated with Alkali, *Ind. Eng. Chem. Res.*, 49, 10836-10844, DOI: 10.1021/ie100407d.
- Kagymanova A. P., Chumachenko V. A., Korotkikh V. N., Kashkin V. N., Noskov A. S., 2011, Catalytic dehydration of bioethanol to ethylene: Pilot-scale studies and process simulation, *Chemical Engineering Journal*, 176, 188-194, DOI: 10.1016/j.cej.2011.06.049.
- Kodama D., Sato R., Haneda A., Kato M., 2005, High-Pressure Phase Equilibrium for Ethylene + Ethanol at 263.15 K, *J. Chem. Eng. Data*, 50, 122-124, DOI: 10.1021/je049796y.
- Luque R., Sze Ki Lin C., Wilson K., Clark J. (Editors), 2016, Handbook of biofuels production, Eds. Woodhead Publishing, Elsevier, Duxford, UK.
- Mohsenzadeh A., Zamani A., Taherzadeh M. J., 2017, Bioethylene Production from Ethanol: A Review and Techno-economical Evaluation, *Chem Bio Eng Rev*, 4, 75-91.
- Paik A. J., Swann S. J., Keyes D. B., 1938, Catalysts for the Equilibrium Ethylene-Water-Ethanol, *Ind. Eng. Chem.*, 30, 173-175, DOI: 10.1021/ie50338a014.
- Phillips C. B., Datta R., 1997, Production of Ethylene from Hydrous Ethanol on H-ZSM-5 under Mild Conditions, *Ind. Eng. Chem. Res.*, 36, 4466-4475.
- Posen I. D., Griffin W. M., Matthews H. S., Azevedo I. L., 2014, Changing the Renewable Fuel Standard to a Renewable Material Standard: Biethylene Case Study, *Environmental Science & Technology*, 49, 93-102, DOI: 10.1021/es503521r.
- Production: Growth is the Norm, 2006, C & En, available on line: <http://pubs.acs.org/cen/coverstory/84/pdf/8428production.pdf> (accessed on 29December 2017).
- Ramis G., Rossetti I., Tripodi A., Compagnoni M., 2017, Diluted bioethanol solutions for the production of hydrogen and ethylene, *Chem. Eng. Trans.*, 57, 1663-1668, DOI: 10.3303/CET1757278.
- Rossetti I., Compagnoni M., De Guido G., Pellegrini L., Ramis G., Dzwigaj S., Ethylene Production from Diluted Bioethanol Solutions, 2017a, *The Canadian Journal of Chemical Engineering*, 95, 1752-1759, DOI: 10.1002/cjce.22828.
- Rossetti, I., Compagnoni M., Finocchio E., Ramis G., Di Michele A., Millot Y., Dzwigaj S., 2017b, Ethylene production via catalytic dehydration of diluted bioethanol: A step towards an integrated biorefinery, *Appl. Cat. B: Environmental*, 210, 407-420, DOI: 10.1016/j.apcatb.2017.04.007.
- Rossetti I., Lasso J., Compagnoni M., De Guido G., Pellegrini L., 2015, *Chem. Eng. Trans.*, 43, 229-234.